

# Probing Quantum Phase Transitions on a Spin Chain with a Double Quantum Dot

Yun-Pil Shim,<sup>1</sup> Sangchul Oh,<sup>2</sup> Jianjia Fei,<sup>1</sup> Xuedong Hu,<sup>2</sup> and Mark Friesen<sup>1</sup>

<sup>1</sup>*Department of Physics, University of Wisconsin-Madison, Madison, Wisconsin 53706, USA*

<sup>2</sup>*Department of Physics, University at Buffalo, State University of New York, Buffalo, New York 14260, USA*

(Dated: January 25, 2023)

Quantum phase transitions (QPTs) in qubit systems are known to produce singularities in the entanglement, which could in turn be used to probe the QPT. Current proposals to measure the entanglement are challenging however, because of their nonlocal nature. Here we show that a double quantum dot coupled locally to a spin chain provides an alternative and efficient probe of QPTs. We propose an experiment to observe a QPT in a triple dot, based on the well-known singlet projection technique.

PACS numbers: 03.67.Lx, 73.21.La, 75.10.Pq, 64.70.Tg, 05.30.Rt, 85.35.Gv

Spin chains have been studied for many years because of their simple formulation, which enables analytical solutions, and their similarity to more complex quantum many-body systems. Recently, it has been possible to engineer fully tunable spin chains based on quantum dots with one or more electrons [1]. Such chains can be used as spin qubits for quantum computing [2], or as a spin bus whose ground state transmits quantum information over large distances [3–6]. In all these settings, the ability to mediate entanglement is paramount for incorporating spin chains into quantum devices.

Quantum phase transitions (QPTs) can have a strong effect on adiabatic operations involving the ground state of a spin chain. QPTs occur at energy level crossings as a function of external parameters, between ground states with very different physical properties [7]. In the critical regime where the two ground states are nearly degenerate, macroscopic observables such as two-qubit entanglement can exhibit non-analytic behavior [8–12]. In finite-size systems, the phase transition is typically discontinuous, or first order; however, the underlying physics is essentially the same as in infinite systems.

From a quantum information perspective, QPTs may produce singularities in the entanglement, which could potentially enhance device operation. Alternately, we could view entanglement as a sensitive probe of the ground state, which could potentially enhance our understanding of QPTs. The latter approach was recently applied to *XY*-type spin chains, using nonlocal pairs of qubits to probe the QPT [13–15]. In this configuration, strong enhancements of the entanglement were observed near critical points. However, in realistic quantum dots, the spin couplings are not of the *XY* type, and nonlocal measurements can be rather challenging [16].

Because of its simplicity, a local probe could potentially be more effective. Unfortunately, the simplest type of measurement – mapping out the effective interaction between the spin chain and a weakly coupled qubit – does not exhibit unusual behavior near an energy level crossing [17]. It has been suggested that the time evolution of a coupled qubit could be used to probe a QPT [18, 19]

via the Loshmidt echo [20]. This method has been successfully implemented using nuclear magnetic resonance (NMR) [21, 22]. Such dynamical methods are powerful, but they are still more challenging than simple projective measurements.

In this Letter, we propose a local, projective scheme for detecting QPTs in a quantum dot spin chain. The chain undergoes successive QPTs as a function of the external magnetic field. We study two different external probes of the QPT. First, we consider a nonlocal probe, consisting of two qubits weakly coupled to the chain at different locations. We calculate the entanglement between the probe qubits numerically, using the concurrence measure [23], and we observe singularities when the spin chain undergoes a QPT. We also obtain analytical estimates for the entanglement using perturbation theory. Next, we consider a local probe, consisting of a double quantum dot coupled to a single node of the spin chain. We find that the ground state properties of the chain are imprinted onto the probe, and we investigate the concurrence singularities both numerically and analytically. Interestingly, we find that the probability for the probe qubits to form a singlet state echos the non-analytic response of the concurrence. This is significant because the singlet probability is relatively easy to measure, using the singlet projection technique common to spin qubit experiments [24]. We propose a simple experiment to test these concepts on the smallest possible spin system of size  $N = 1$ . This “chain” has a single energy level crossing as a function of magnetic field, and the ground state transition exhibits a non-analyticity consistent with a QPT. Our proposal involves a total of three quantum dots, and it is therefore within reach of current triple dot technologies [25–27].

*Energy level crossings in the spin chain.*—We adopt an isotropic Heisenberg model of a spin chain, as appropriate for single-electron spins in quantum dots. The Hamiltonian for a chain of length  $N$  is given by  $H_c = J_c \sum_{j=1}^{N-1} \mathbf{s}_j \cdot \mathbf{s}_{j+1} - B_c \sum_{j=1}^N s_{jz}$  where  $\mathbf{s}_j$  are spin operators for the individual electrons. The bare exchange couplings between the spins are labelled  $J_c$ , and the ap-

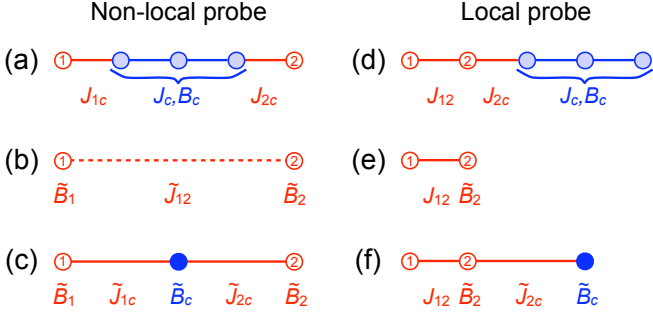


FIG. 1. Graphical representations of the Hamiltonians studied here. (a)-(c) correspond to a nonlocal probe in which the probe qubits (1 and 2) are attached to different nodes on the spin chain. (d)-(f) correspond to a local probe in which a pair of qubits is attached to a single node on the chain. (a) and (d) describe the full, physical geometry, where the chain (lightly shaded circles) is formed of an arbitrary number of physical spins. Here, we show probe qubits attached to the endpoints of the chain; however, similar results are obtained for any attachment points. (b), (c), (e), and (f) represent effective geometries, in which the spin chain in its ground state is replaced by a pseudospin, as indicated by a filled circle (when appropriate). (b) and (e) represent non-critical Hamiltonians (far away from a critical point), where the bus ground state is non-degenerate (pseudospin-0). (c) and (f) represent critical Hamiltonians, where the bus ground state is doubly-degenerate (pseudospin-1/2). In the effective Hamiltonians, the bus pseudospin interacts with the probe qubits via effective couplings ( $\tilde{J}$ ) and effective fields ( $\tilde{B}$ ). In (b), the effective coupling  $\tilde{J}_{12}$  is weak (*i.e.*, second order), as indicated by a dashed line.

plied magnetic field is  $\mathbf{B}_c = B_c \hat{\mathbf{z}}$ . Throughout this paper, we will adopt  $J_c$  as the unit of energy. Magnetic fields will also be expressed in energy units. A pictorial representation of the chain Hamiltonian is given by the lightly shaded circles in Figs. 1(a) and (d). For now, we ignore any couplings to external qubits, and calculate the energy spectrum for  $H_c$  as a function of  $B_c$ . The results are shown in Figs. 2(a) and (b) for the cases  $N = 4$  and 5. In this letter, we are most interested in the two lowest energy levels for a given  $B_c$ , whose crossings are indicated by circles in Fig. 2. Each level crossing is associated with a QPT in the finite-size spin chain.

*Nonlocal probe.*—Next, we consider external qubits, labelled 1 and 2 in Figs. 1(a) and (d), which will serve as probes of the QPT. The probe coupling Hamiltonian is given by  $H_p = J_{1c} \mathbf{S}_1 \cdot \mathbf{s}_1 + J_{2c} \mathbf{S}_2 \cdot \mathbf{s}_N$  where  $\mathbf{S}_j$  are the spin operators for the probe qubits. The probes may be coupled to any node of the spin chain, with similar results. For definiteness here, we have attached them to the endpoints of the chain.

When the probe couplings are turned on, the energy levels of the chain expand into energy manifolds. Our goal is to probe the QPT without disturbing it, so the manifold structure in Figs. 2(a) and (b) should remain

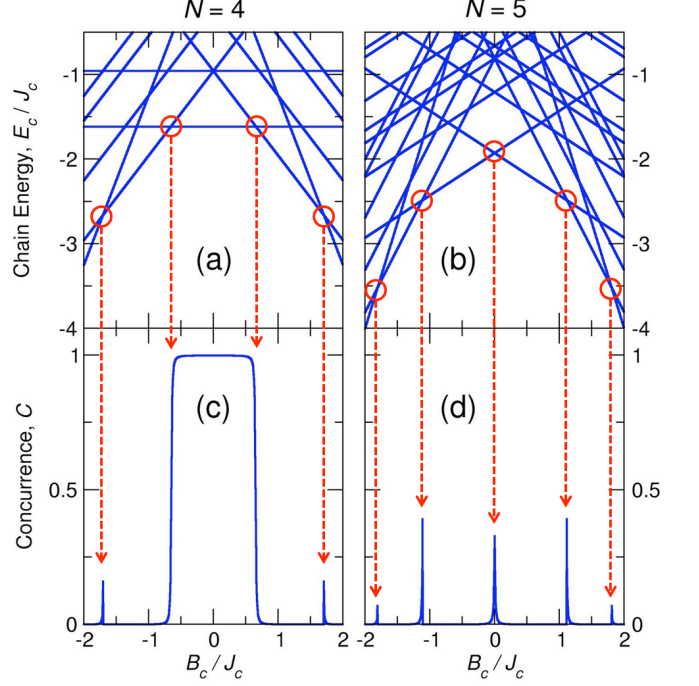


FIG. 2. (a), (b) Energy spectra of spin chains of length  $N = 4$  and 5, with no coupled qubits, as a function of the magnetic field  $B_c$  expressed in energy units, and scaled by the coupling constant  $J_c$ . The energy level crossings of the ground state are indicated by circles. (c), (d) The corresponding concurrence between the probe qubits, when they are coupled in the geometry of Fig. 1(a). Here,  $C$  is dimensionless, and we take  $J_{1c} = J_{2c} = 0.02 J_c$ . The singular features of the concurrence occur at energy level crossings of the chain.

largely undisturbed. This places constraints on the probe couplings. First, the bare coupling constants must be small, such that  $J_{1c}, J_{2c} \ll J_c$ . The magnetic field applied to the probes should also be much smaller than  $J_c$ , necessitating a magnetic field gradient between the qubits and the chain. For definiteness, we take the magnetic field on the probe qubits to be zero. Although large field gradients are difficult to achieve in the laboratory, we will focus on QPTs occurring at zero field, in an odd-size chain. For this case, the field gradient is small, and does not pose a serious experimental challenge.

Figures 2(c) and (d) show the concurrence between the probe qubits. The calculation is performed after first tracing out the spin-chain degrees of freedom from the full Hamiltonian,  $H = H_c + H_p$ , to obtain the reduced, bipartite density matrix. The concurrence exhibits singularities which are correlated with the energy level crossings of the spin chain, as expected for QPTs. Away from the level crossings, the concurrence falls quickly to zero. The only exception to this regular behavior is observed near zero field for even-size chains, where the concurrence plateaus at its maximum value,  $C = 1$ .

This interesting behavior can be understood intuitively

by treating the probe qubits as a perturbation. It has previously been shown that when the bare qubit-chain coupling is small, and when the chain is in its ground state, the interactions can be described by an effective Hamiltonian [17]. Far away from a QPT, the system is noncritical and the effective Hamiltonian involves only the external spins, as shown in Fig. 1(b):

$$\tilde{H}_{\text{nc}} = \tilde{B}_1 S_{1z} + \tilde{B}_2 S_{2z} + \sum_{\alpha=x,y,z} \tilde{J}_{12\alpha} S_{1\alpha} S_{2\alpha} . \quad (1)$$

Here, the bare coupling parameters  $J_{1c}$  and  $J_{2c}$  are hidden inside the effective coupling  $\tilde{J}_{12}$  and the effective local fields  $\tilde{B}_{1,2}$ . Note that the effective couplings are generally anisotropic, except in special cases. If the qubit couplings are turned on adiabatically, the chain will remain in an inert, effective pseudospin-0 state. The effective coupling arises due to virtual excitations of the chain outside its ground-state manifold; it is therefore second order in the perturbation:  $\tilde{J}_{12}/J_c \sim (J_{1c}/J_c)^2$ . On the other hand, the effective fields emerge at first order:  $\tilde{B}_{1,2}/J_c \sim (J_{1c,2c}/J_c)^1$ . (Analytical expressions for both quantities are provided in [17] and [28].) We therefore generally find that  $\tilde{B}_{1,2} \gg \tilde{J}_{12}$  in the noncritical regime. Hence, the external qubits align with the effective field to form a separable state, for which  $C \simeq 0$ . The only exception is the special case near  $B_c = 0$  for an even-size chain. Here  $\tilde{B}_{1,2} = 0$  due to the spin-singlet character of the chain ground state. Since  $\tilde{J}_{12} \neq 0$ , it can generate maximal entanglement between the probe qubits, as indicated in Fig. 2(c).

The situation is very different near a QPT. In this case, the ground state of the chain is approximately two-fold degenerate and behaves as an effective pseudospin-1/2, as shown in Fig. 1(c). The effective Hamiltonian at the critical point then describes a simple three-body system:

$$\tilde{H}_{\text{cp}} = \tilde{H}_{\text{nc}} - \tilde{B}_c S_{cz} + \sum_{\alpha=x,y,z} \left( \tilde{J}_{1c\alpha} S_{1\alpha} S_{c\alpha} + \tilde{J}_{2c\alpha} S_{2\alpha} S_{c\alpha} \right) . \quad (2)$$

Here, the spin operator  $\mathbf{S}_c$  acts on the the pseudospin-1/2 of the chain ground state. In contrast with the noncritical regime, the effective couplings are now first order in the perturbation:  $\tilde{J}_{1c,2c}/J_c \sim J_{1c,2c}/J_c$ . Because  $\tilde{J}_{1c,2c}$  are relatively large,  $\tilde{H}_{\text{cp}}$  can mediate entanglement between the two probe qubits, with the resulting value of the concurrence determined by the relative size of  $\tilde{J}_{1c,2c}$  compared to  $\tilde{B}_{1,2}$ . The couplings  $\tilde{J}_{1c,2c}$  enhance entanglement while the fields  $\tilde{B}_{1,2}$  suppress it.

We can take this analysis further for the QPT occurring at  $B_c = 0$  in an odd-size spin chain [*e.g.*, the central peak in Fig. 2(d)]. In this case, the effective Hamiltonian has a much simpler, isotropic form, with  $\tilde{J}_{1c} = \tilde{J}_{2c} = \tilde{J}$ ,  $\tilde{B}_{1,2} = 0$ ,  $\tilde{B}_c = B_c$ , and  $\tilde{H}_{\text{cp}} = \tilde{J}(\mathbf{S}_1 + \mathbf{S}_2) \cdot \mathbf{S}_c - B_c S_{c,z}$ . We can derive an expression for the concurrence between the probe qubits which shows the explicit form of the

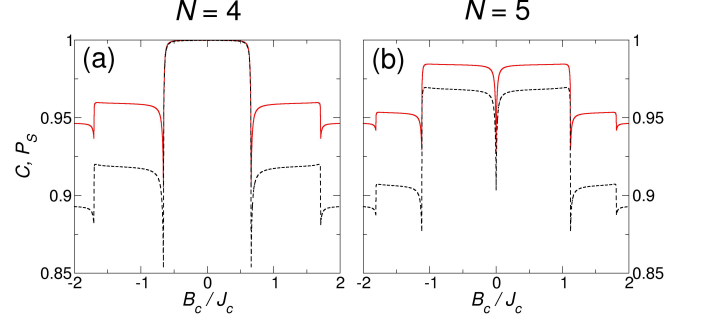


FIG. 3. The concurrence  $C$  and singlet probability  $P_S$  (dashed black and solid red curves, respectively) of a double-dot, local probe coupled to a spin chain of size (a)  $N = 4$  and (b)  $N = 5$ , as the chain undergoes QPTs. Here we take  $J_{12}=J_{2c}=0.02J_c$ .  $C$  and  $P_S$  are both dimensionless.

non-analyticity [28]:

$$C = \frac{1}{2} \left[ 1 - \frac{|B_c| + \tilde{J}/2}{\sqrt{B_c^2 + \frac{9}{4}\tilde{J}^2 + \tilde{J}|B_c|}} \right] . \quad (3)$$

We see that the concurrence attains a maximum value of  $1/3$  at the critical point [29], and decreases to zero as  $(J_c/B_c)^2$  when  $B_c \gtrsim J_c$ . The full-width-at-half-max of the peak is given by  $(-1 + \sqrt{32/5})\tilde{J} \simeq 1.53\tilde{J}$ .

We close this section by describing an experimental procedure for observing concurrence peaks associated with QPTs in a spin chain. The spin system is prepared in its ground state via thermalization, or an adiabatic initialization procedure. The concurrence measurement requires performing full quantum state tomography of the two-qubit reduced density matrix. This involves 15 separate measurements of the two-qubit correlators  $\{\sigma_{1i}\sigma_{2j}\}$ , where  $\sigma_{1i}$  ( $\sigma_{2j}$ ) is a Pauli operator acting on qubit 1 (2), with  $i, j \in \{I, X, Y, Z\}$  [30]. (We exclude the trivial two-qubit identity operator.)

*Local probe.*—The local probe geometry that we consider is shown in Fig. 1(d). Here, one side of a double-quantum dot is attached to one node of a spin chain. In this case, the probe Hamiltonian is given by  $H_p = J_{12}\mathbf{S}_1 \cdot \mathbf{S}_2 + J_{2c}\mathbf{S}_2 \cdot \mathbf{S}_1$ . Using the methods described above, we can compute the concurrence between the spins in the probe double dot, obtaining the results shown in Fig. 3, for two different size chains. We find that the QPTs occurring in the chain are imprinted onto the probe. In Fig. 3, we also show the overlap probability  $P_S$  between the probe qubits and a singlet state. We see that  $P_S$  mirrors the singularity in  $C$ .

We can understand the main features in Fig. 3 by applying perturbation theory to the local probe geometry. As before, the chain is effectively inert away from a critical point, and the noncritical effective Hamiltonian is given by

$$\tilde{H}_{\text{nc}} = \tilde{B}_2 S_{2,z} + J_{12}\mathbf{S}_1 \cdot \mathbf{S}_2 . \quad (4)$$

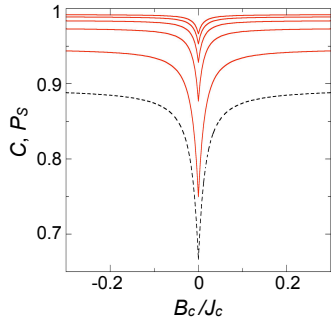


FIG. 4. Solid red curves show the singlet probabilities  $P_S$  for a double quantum dot coupled locally to a spin chain of length  $N$ , as a function of the magnetic field on the chain. From top to bottom, the curves correspond to  $N = 9, 7, 5, 3$ , and  $1$ . The dashed black curve shows the corresponding concurrence  $C$  for the case  $N = 1$ . Here, we take  $J_{12} = J_{2c} = 0.02J_c$ .

The entanglement between the probe qubits is determined by the interplay between  $J_{12}$  which enhances the concurrence, and  $\tilde{B}_2$  which suppresses it. The effective local field,  $\tilde{B}_2 = \langle 0 | s_{1z} | 0 \rangle$ , depends only on the true spin of the ground state of the spin chain,  $| 0 \rangle$ . In contrast with the pseudospin, which remains fixed at 0, the true spin increases by 1 in each successive noncritical region, away from  $B_c = 0$ . Accordingly, the concurrence is suppressed in discrete steps.

Approaching a critical point, the chain becomes pseudospin-1/2, and the effective Hamiltonian becomes

$$\tilde{H}_{\text{cp}} = \tilde{H}_{\text{nc}} - \tilde{B}_c S_{cz} + \sum_{\alpha=x,y,z} \tilde{J}_{2\alpha} S_{2\alpha} S_{c\alpha} . \quad (5)$$

The singularities all have a downward-pointing “valley” shape, which can be explained by considering the  $B_c=0$  transition in Fig. 3(b). In the non-critical region,  $\tilde{B}_2 \neq 0$ , while in the critical region,  $\tilde{B}_2=0$  (the latter is only true for the  $B_c=0$  transition [28]). This would normally lead to an upward-pointing singularity, since  $\tilde{B}_2$  suppresses the entanglement. However, a second effective coupling ( $\tilde{J}_{2c}$ ) emerges in the critical region, as indicated in Eq. (5), which reduces the entanglement between qubits 1 and 2 by sharing the entanglement with pseudospin  $c$ . We now show that the latter effect is always dominant, leading to valley-type singularities, by obtaining exact solutions for the asymptotic critical and noncritical behaviors.

We focus strictly on the  $B_c=0$  transitions in odd-size spin chains. Figure 4 shows several  $B_c=0$  transitions for chains of varying length. At the special point  $B_c=0$ , we find that  $\tilde{B}_c=\tilde{B}_2=0$ , and the effective coupling  $\tilde{J}_{2c}$  is isotropic, yielding the effective Hamiltonian  $\tilde{H}_{\text{cp}} = (J_{12}\mathbf{S}_1 + \tilde{J}_{2c}\mathbf{S}_c) \cdot \mathbf{S}_2$ . Since  $C$  and  $P_S$  are dimensionless quantities, at the point  $B_c=0$  they can only be functions of the dimensionless ratio  $\gamma = \tilde{J}_{2c}/J_{12}$ . From

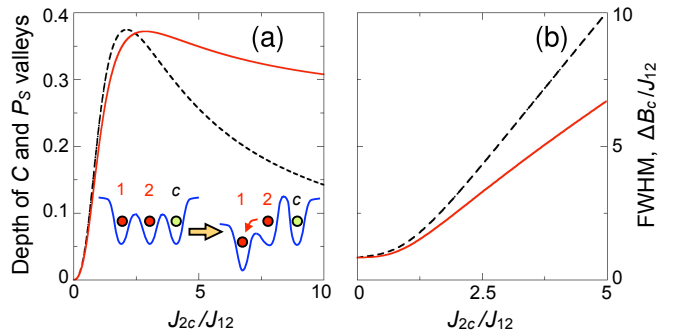


FIG. 5. (a) Depth of  $C$  and  $P_S$  valley singularities, like those shown in Fig. 4 (with  $N = 1$ ), when two probe qubits (1 and 2) are coupled to a quantum dot ( $c$ ), plotted as a function of the coupling ratio. The inset shows the confinement profile of the triple-dot experiment. (b) Full-width-at-half-minimum (FWHM) of the valleys with  $J_{12}$  fixed at  $0.02J_c$ . In both panels, the concurrence  $C$  and the singlet probability  $P_S$  are represented by dashed black and solid red curves, respectively.

Eq. (5) we obtain [28]

$$C = \frac{1}{3} \left( 1 + \frac{2 - \gamma}{\sqrt{1 - \gamma + \gamma^2}} \right), \quad P_S = (1 + 3C)/4 . \quad (6)$$

The concurrence  $C$  was also obtained numerically for this special case in Ref. [29].

Far away from a critical point, Eq. (4) is valid, so  $C$  and  $P_S$  can only be functions of the dimensionless ratio  $\tilde{B}_2/J_{12}$ . However, it can also be shown that  $\tilde{B}_2/J_{12} = \tilde{J}_{2c}/2J_{12} = \gamma/2$  for the  $B_c = 0$  transition [28], leading to

$$C = 1/\sqrt{1 + \gamma^2/4}, \quad P_S = (1 + C)/2 , \quad (7)$$

in this limit. We have also solved for the critical behavior in more general cases, as described in [28], although the expressions are more complicated.

In the limit of large chain size,  $N \gg 1$ , we have previously shown that  $\gamma \rightarrow 0$  as  $\sim N^{-1/2}$  [5, 31]. Hence,  $C$  and  $P_S$  approach the constant value of 1, and the singularity is suppressed, as consistent with Fig. 4. Using Eqs. (6) and (7), we can define the depths of the  $C$  and  $P_S$  valleys as the difference between their asymptotic values at large and small  $B_c$ . In the limit of  $\gamma \rightarrow 0$ , we find that the  $C$  and  $P_S$  valley depths approach zero quickly, as  $\gamma^2/8 \sim 1/N$ .

*Triple-dot experiment.*—We now propose an experiment to investigate the QPT in the opposite limit,  $N = 1$ . We consider the triple quantum dot geometry shown in the inset of Fig. 5(a). For simplicity, we assume the dots are singly occupied. The double quantum dot (on the left) is used to probe a spin “chain” of length 1 (on the right), whose ground state properties change dramatically as a function of the applied field  $B_c$  at the transition point  $B_c = 0$ . The field is applied only to spin  $c$ , necessitating a gradient scheme to cancel out the field on the

probe dots. The experiment proceeds by first preparing the triple dot in its ground state. We then turn off the exchange coupling to dot  $c$  and detune the probe double dot, so that the electron in dot 2 moves to dot 1 only when the probe is in a singlet state, due to the large singlet-triplet energy splitting [24]. The singlet probability can then be monitored using charge sensing, via a nearby charge sensor.

For the case  $N = 1$ , it can be shown that  $\tilde{B}_2 = \pm J_{2c}/2$  in Eq. (4) [28], so  $\gamma = J_{2c}/J_{12}$ . We can then determine the depth of the  $C$  and  $P_S$  valleys, as well as their widths, as a function of this ratio, as shown in Fig. 5. Generally, we see that applied fields of order  $B_c \sim J_{12}$  are needed, to observe the QPT. Since quantum dot exchange couplings are typically of order  $\mu\text{eV}$ , the magnetic field differences between the quantum dots needed in this experiment are of order 10 mT, and relatively easy to achieve in the laboratory [32].

*Summary and conclusions.*—In summary, we have shown that QPTs in a quantum dot spin chain cause non-analytic behavior in the entanglement between qubits attached to the chain locally or nonlocally, and we have argued that there are benefits to using a local probe. Based on these methods, we proposed an experimental protocol for observing a QPT in a triple quantum dot. Although we do not describe the results here, we have also found that QPTs can be observed in other types of spin chains (*e.g.*,  $XY$ ), using a local probe. We believe that the local probe could be very useful for investigating entanglement in many quantum dot geometries, because of the practicality of performing singlet projection measurements.

This work was supported by the DARPA QuEST program through a grant from AFOSR, and by NSA/LPS through grants from ARO (W911NF-08-1-0482 and W911NF-09-1-0393).

- 
- [1] L. Jacak, P. Hawrylak, and A. Wojs, *Quantum Dots* (Springer-Verlag, Berlin, 1998).  
[2] D. Loss and D. P. DiVincenzo, Phys. Rev. A **57**, 120 (1998).  
[3] Y. Li, T. Shi, B. Chen, Z. Song, and C.-P. Sun, Phys. Rev. A **71**, 022301 (2005).  
[4] L. C. Venuti, C. D. E. Boschi, and M. Roncaglia, Phys. Rev. Lett. **96**, 247206 (2006).  
[5] M. Friesen, A. Biswas, X. Hu, and D. Lidar, Phys. Rev. Lett. **98**, 230503 (2007).  
[6] S. Oh, L.-A. Wu, Y.-P. Shim, J. Fei, M. Friesen, and X. Hu, Phys. Rev. A **84**, 022330 (2011).  
[7] S. Sachdev, *Quantum Phase Transitions* (Cambridge University Press, 1999).  
[8] A. Osterloch, L. Amico, G. Falci, and R. Fazio, Nature (London) **416**, 608 (2002).  
[9] T. J. Osborne and M. A. Nielsen, Phys. Rev. A **66**, 032110 (2002).  
[10] G. Vidal, J. I. Latorre, E. Rico, and A. Kitaev, Phys.

- Rev. Lett. **90**, 227902 (2003).  
[11] S.-J. Gu, H.-Q. Lin, and Y.-Q. Li, Phys. Rev. A **68**, 042330 (2003).  
[12] F. Pollmann, S. Mukerjee, A. M. Turner, and J. E. Moore, Phys. Rev. Lett. **102**, 255701 (2009).  
[13] X. X. Yi, H. T. Cui, and L. C. Wang, Phys. Rev. A **74**, 054102 (2006).  
[14] Z.-G. Yuan, P. Zhang, and S.-S. Li, Phys. Rev. A **76**, 042118 (2007).  
[15] Q. Ai, T. Shi, G. Long, and C. P. Sun, Phys. Rev. A **78**, 022327 (2008).  
[16] M. D. Shulman, O. E. Dial, S. P. Harvey, H. Bluhm, V. Umansky, and A. Yacoby, Science **336**, 202 (2012).  
[17] Y.-P. Shim, S. Oh, X. Hu, and M. Friesen, Phys. Rev. Lett. **106**, 180503 (2011).  
[18] H. T. Quan, Z. Song, X. F. Liu, P. Zanardi, and C. P. Sun, Phys. Rev. Lett. **96**, 140604 (2006).  
[19] Z.-G. Yuan, P. Zhang, and S.-S. Li, Phys. Rev. A **75**, 012102 (2007).  
[20] T. Gorin, T. Prosen, T. H. Seligman, and M. Žnidarič, Phys. Rep. **435**, 33 (2006).  
[21] J. Zhang, X. Peng, N. Rajendran, and D. Suter, Phys. Rev. Lett. **100**, 100501 (2008).  
[22] J. Zhang, F. M. Cucchietti, C. M. Chandrashekar, M. Laforest, C. A. Ryan, M. Ditty, A. Hubbard, J. K. Gamble, and R. Laflamme, Phys. Rev. A **79**, 012305 (2009).  
[23] W. K. Wootters, Phys. Rev. Lett. **80**, 2245 (1998).  
[24] J. R. Petta, A. C. Johnson, J. M. Taylor, E. A. Laird, A. Yacoby, M. D. Lukin, C. M. Marcus, M. P. Hanson, and A. C. Gossard, Science **309**, 2180 (2005).  
[25] D. Schröer, A. D. Greentree, L. Gaudreau, K. Eberl, L. C. L. Hollenberg, J. P. Kotthaus, and S. Ludwig, Phys. Rev. B **76**, 075306 (2007).  
[26] S. Amaha, T. Hatano, H. Tamura, S. Teraoka, T. Kubo, Y. Tokura, D. G. Austing, and S. Tarucha, Phys. Rev. B **85**, 081301(R) (2012).  
[27] L. Gaudreau, G. Granger, A. Kam, G. C. Aers, S. A. Studenikin, P. Zawadzki, M. Pioro-Ladrière, Z. R. Wasilewski, and A. S. Sachrajda, Nat. Phys. **8**, 54 (2012).  
[28] See Supplemental material.  
[29] S. Oh, M. Friesen, and X. Hu, Phys. Rev. B **82**, 140403(R) (2010).  
[30] M. A. Nielsen and I. L. Chuang, *Quantum Computation and Quantum Information* (Cambridge University Press, Cambridge, United Kingdom, 2000).  
[31] S. Oh, Y.-P. Shim, J. Fei, M. Friesen, and X. Hu, Phys. Rev. B **85**, 224418 (2012).  
[32] M. Pioro-Ladrière, T. Obata, Y. Tokura, Y.-S. Shin, T. Kubo, K. Yoshida, T. Taniyama, and S. Tarucha, Nature Phys. **4**, 776 (2008).

## SUPPLEMENTAL MATERIAL

Here we provide detailed derivations of analytical expressions for the concurrence  $C$  and the singlet probability  $P_S$  near the critical transition at  $B_c = 0$  in an odd-size chain, as reported in the main text. For completeness, we also provide expressions for the effective couplings  $\tilde{J}$  and local fields  $\tilde{B}$ , as originally derived in Ref. [17]

### Expressions for effective couplings and local fields

The following formulae, used in the main text, were first derived in Ref. [17].

For the nonlocal probe in the noncritical regime [Eq. (1) of the main text]:

$$\tilde{B}_1 = J_{1c} \langle 0 | s_{1z} | 0 \rangle , \quad (1)$$

$$\tilde{B}_2 = J_{2c} \langle 0 | s_{Nz} | 0 \rangle , \quad (2)$$

$$\tilde{J}_{12\alpha} = -2 \sum_{m>0} \frac{J_{1c} J_{2c}}{\varepsilon_m - \varepsilon_0} \langle 0 | s_{1\alpha} | m \rangle \langle m | s_{N\alpha} | 0 \rangle \quad (\text{for } \alpha = x, y, z) . \quad (3)$$

Here  $|m\rangle$  corresponds to the  $m$ -th eigenstate of the spin chain Hamiltonian,  $H_c$ , with energy  $\varepsilon_m$ . Here,  $m = 0$  corresponds to the unique ground state.

For the nonlocal probe in the critical regime [Eq. (2) of the main text], we define the pseudospin “up” state ( $|\uparrow\rangle$ ) and “down” state ( $|\downarrow\rangle$ ) as the ground states of the spin chain on either side of the transition, for higher and lower magnetic fields, respectively. The effective variables are

$$\tilde{B}_1 = \frac{J_{1c}}{2} (\langle \uparrow | s_{1z} | \uparrow \rangle + \langle \downarrow | s_{1z} | \downarrow \rangle) , \quad (4)$$

$$\tilde{B}_2 = \frac{J_{2c}}{2} (\langle \uparrow | s_{Nz} | \uparrow \rangle + \langle \downarrow | s_{Nz} | \downarrow \rangle) , \quad (5)$$

$$\tilde{B}_c = \varepsilon_{\downarrow} - \varepsilon_{\uparrow} , \quad (6)$$

$$\tilde{J}_{12\alpha} = -J_{1c} J_{2c} \sum_{m \neq \uparrow, \downarrow} \left[ \frac{\langle \uparrow | | s_{1\alpha} | m \rangle \langle m | s_{N\alpha} | \uparrow \rangle}{\varepsilon_m - \varepsilon_{\uparrow}} + \frac{\langle \downarrow | | s_{1\alpha} | m \rangle \langle m | s_{N\alpha} | \downarrow \rangle}{\varepsilon_m - \varepsilon_{\downarrow}} \right] \quad (\text{for } \alpha = x, y, z) , \quad (7)$$

$$\tilde{J}_{1c\alpha} = \begin{cases} J_{1c} \langle \uparrow | s_{1+} | \downarrow \rangle & (\text{for } \alpha = x, y) , \\ J_{1c} (\langle \uparrow | s_{1z} | \uparrow \rangle - \langle \downarrow | s_{1z} | \downarrow \rangle) & (\text{for } \alpha = z) , \end{cases} \quad (8)$$

$$\tilde{J}_{2c\alpha} = \begin{cases} J_{2c} \langle \uparrow | s_{N+} | \downarrow \rangle & (\text{for } \alpha = x, y) , \\ J_{2c} (\langle \uparrow | s_{Nz} | \uparrow \rangle - \langle \downarrow | s_{Nz} | \downarrow \rangle) & (\text{for } \alpha = z) . \end{cases} \quad (9)$$

For the local probe in the noncritical regime [Eq. (4) of the main text]

$$\tilde{B}_2 = J_{2c} \langle 0 | s_{1z} | 0 \rangle . \quad (10)$$

For the local probe in the critical regime [Eq. (5) of the main text]

$$\tilde{B}_2 = \frac{J_{2c}}{2} (\langle \uparrow | s_{1z} | \uparrow \rangle + \langle \downarrow | s_{1z} | \downarrow \rangle) , \quad (11)$$

$$\tilde{B}_c = \varepsilon_{\downarrow} - \varepsilon_{\uparrow} , \quad (12)$$

$$\tilde{J}_{2c\alpha} = \begin{cases} J_{2c} \langle \uparrow | s_{1+} | \downarrow \rangle & (\text{for } \alpha = x, y) , \\ J_{2c} (\langle \uparrow | s_{1z} | \uparrow \rangle - \langle \downarrow | s_{1z} | \downarrow \rangle) & (\text{for } \alpha = z) . \end{cases} \quad (13)$$

### Concurrence of a nonlocal probe

In this section, we derive Eq. (3) of the main text, which describes the concurrence of a nonlocal probe coupled to a pseudospin in the critical regime near the  $B_c = 0$  transition. The pseudospin effective Hamiltonian is given by

$$\tilde{H}_{\text{cp}} = \tilde{J} (\mathbf{S}_1 + \mathbf{S}_2) \cdot \mathbf{S}_c - \tilde{B}_c S_{c,z} . \quad (14)$$

Without loss of generality, we will only consider  $\tilde{B}_c \geq 0$ .  $S_{\text{tot},z} = S_{1,z} + S_{2,z} + S_{c,z}$  and  $S_{12}^2 = (\mathbf{S}_1 + \mathbf{S}_2)^2$  are good quantum numbers. For the subspace with  $S_{\text{tot},z} = \pm 3/2$  and  $S_{12} = 1$ , the eigenstates are  $|S_{1,z}, S_{c,z}, S_{2,z}\rangle = |\uparrow\uparrow\uparrow\rangle$  and  $|\downarrow\downarrow\downarrow\rangle$ , respectively. The eigenenergies are  $E_{\pm 3/2} = \tilde{J}/2 \mp \tilde{B}_c/2$ . For  $S_{\text{tot},z} = 1/2$  and  $S_{12} = 0$ , the eigenstate is  $(|\uparrow\uparrow\downarrow\rangle - |\downarrow\uparrow\uparrow\rangle)/\sqrt{2}$  and the eigenenergy is  $-\tilde{B}_c/2$ . For  $S_{\text{tot},z} = 1/2$  and  $S_{12} = 1$ , the subspace is two-dimensional, and in the ordered basis  $\{|\uparrow\downarrow\uparrow\rangle, (|\uparrow\uparrow\downarrow\rangle + |\downarrow\uparrow\uparrow\rangle)/\sqrt{2}\}$  we have

$$H_{1/2} = \begin{pmatrix} \frac{\tilde{B}_c - \tilde{J}}{2} & \frac{\sqrt{2}}{2} \tilde{J} \\ \frac{\sqrt{2}}{2} \tilde{J} & -\frac{\tilde{B}_c}{2} \end{pmatrix}. \quad (15)$$

The lowest eigenvalue in this subspace is  $E_{1/2} = -\tilde{J}/4 - A_{1/2}/2$ , where  $A_{1/2} = \sqrt{\frac{9}{4}\tilde{J}^2 + \tilde{B}_c^2 - \tilde{J}\tilde{B}_c}$ . For  $S_{\text{tot},z} = -1/2$  and  $S_{12} = 0$ , the eigenstate is  $(|\uparrow\downarrow\downarrow\rangle - |\downarrow\downarrow\uparrow\rangle)/\sqrt{2}$  and the eigenenergy is  $\tilde{B}_c/2$ . For  $S_{\text{tot},z} = -1/2$  and  $S_{12} = 1$ , the subspace is two-dimensional, and in the ordered basis  $\{(|\uparrow\downarrow\downarrow\rangle + |\downarrow\downarrow\uparrow\rangle)/\sqrt{2}, |\downarrow\uparrow\downarrow\rangle\}$  we have

$$H_{-1/2} = \begin{pmatrix} \frac{\tilde{B}_c}{2} & \frac{\sqrt{2}}{2} \tilde{J} \\ \frac{\sqrt{2}}{2} \tilde{J} & -\frac{\tilde{B}_c + \tilde{J}}{2} \end{pmatrix}. \quad (16)$$

The lowest eigenvalue in this subspace is  $E_{-1/2} = -\tilde{J}/4 - A_{-1/2}/2$ , where  $A_{-1/2} = \sqrt{\frac{9}{4}\tilde{J}^2 + \tilde{B}_c^2 + \tilde{J}\tilde{B}_c}$ .

When  $\tilde{B}_c \geq 0$ , we can easily see that  $E_{-1/2}$  is the ground state energy, and its eigenstate is given by

$$|\Psi_{\text{GS}}\rangle = \frac{1}{\sqrt{2}} \left( \cos \frac{\theta}{2} |\uparrow\downarrow\downarrow\rangle + \sin \frac{\theta}{2} |\downarrow\downarrow\uparrow\rangle \right), \quad (17)$$

where  $\theta$  is defined in the range  $0 \leq \theta \leq \pi$  by

$$\cos \theta = -\frac{\frac{\tilde{J}}{2} + \tilde{B}_c}{A_{-1/2}}, \quad (18)$$

$$\sin \theta = \frac{\sqrt{2}\tilde{J}}{A_{-1/2}}. \quad (19)$$

We can construct the eight-dimensional density matrix for the ground state and trace out the pseudospin degree of freedom. The resulting reduced density matrix for the probe qubits is then given by

$$\rho = \frac{1}{2} \cos^2 \frac{\theta}{2} (|\uparrow\downarrow\rangle\langle\uparrow\downarrow| + |\downarrow\uparrow\rangle\langle\downarrow\uparrow| + |\uparrow\downarrow\rangle\langle\uparrow\downarrow| + |\downarrow\uparrow\rangle\langle\downarrow\uparrow|) + \sin^2 \frac{\theta}{2} |\downarrow\downarrow\rangle\langle\downarrow\downarrow| \quad (20)$$

$$= \begin{pmatrix} 0 & 0 & 0 & 0 \\ 0 & \frac{1}{2} \cos^2 \frac{\theta}{2} & \frac{1}{2} \cos^2 \frac{\theta}{2} & 0 \\ 0 & \frac{1}{2} \cos^2 \frac{\theta}{2} & \frac{1}{2} \cos^2 \frac{\theta}{2} & 0 \\ 0 & 0 & 0 & \sin^2 \frac{\theta}{2} \end{pmatrix}. \quad (21)$$

The concurrence is defined as [23]  $C = \max\{0, \sqrt{\varepsilon_1} - \sqrt{\varepsilon_2} - \sqrt{\varepsilon_3} - \sqrt{\varepsilon_4}\}$ , where  $\varepsilon_1 \geq \varepsilon_2 \geq \varepsilon_3 \geq \varepsilon_4 \geq 0$  are the eigenvalues of the operator  $R = \rho (\sigma_y \otimes \sigma_y) \rho^* (\sigma_y \otimes \sigma_y)$ , and  $\sigma_y$  is a Pauli spin matrix. From Eq. (21), we then obtain

$$C = \cos^2 \frac{\theta}{2} = \frac{1}{2} \left( 1 - \frac{\frac{\tilde{J}}{2} + \tilde{B}_c}{A_{-1/2}} \right) = \frac{1}{2} \left( 1 - \frac{\frac{\tilde{J}}{2} + \tilde{B}_c}{\sqrt{\frac{9}{4}\tilde{J}^2 + \tilde{B}_c^2 + \tilde{J}\tilde{B}_c}} \right). \quad (22)$$

### Concurrence and singlet probability of a local probe connected to an odd-size spin chain

In this section, we first derive Eq. (7) of the main text, which describes the concurrence and singlet probability of a local probe coupled to a pseudospin in the noncritical regime near the  $B_c = 0$  transition. From Eq. (4) of the main text,

$$\tilde{H}_{\text{nc}} = \tilde{B}_2 S_{2,z} + J_{12} \mathbf{S}_1 \cdot \mathbf{S}_2. \quad (23)$$

$S_{\text{tot},z}$  is a good quantum number. We readily obtain the two eigenstates  $|\uparrow\uparrow\rangle, |\downarrow\downarrow\rangle$ , corresponding to  $S_{\text{tot},z} = \pm 1$  with eigenvalues  $E_{\pm 1} = J_{12}/4 \pm \tilde{B}_2/2$ . In the subspace of  $S_{\text{tot},z} = 0$ , the Hamiltonian matrix in the basis  $\{|\uparrow\downarrow\rangle, |\downarrow\uparrow\rangle\}$  is given by

$$H_0 = \begin{pmatrix} \frac{-J_{12}}{4} - \frac{\tilde{B}_2}{2} & \frac{J_{12}}{2} \\ \frac{J_{12}}{2} & \frac{-J_{12}}{4} + \frac{\tilde{B}_2}{2} \end{pmatrix}. \quad (24)$$

The lowest eigenvalue in this subspace is  $E_0 = -J_{12}/4 - \sqrt{J_{12}^2 + \tilde{B}_2^2}/2$  and the eigenstate is  $|\Psi_0\rangle = \cos \frac{\theta}{2} |\uparrow\downarrow\rangle - \sin \frac{\theta}{2} |\downarrow\uparrow\rangle$ , where  $\theta$  is defined in the range  $0 \leq \theta \leq \pi$  by

$$\cos \theta = \sqrt{\frac{1 + \tilde{B}_2/\sqrt{J_{12}^2 + \tilde{B}_2^2}}{2}}, \quad (25)$$

$$\sin \theta = \sqrt{\frac{1 - \tilde{B}_2/\sqrt{J_{12}^2 + \tilde{B}_2^2}}{2}}. \quad (26)$$

We can easily verify that  $|\Psi_0\rangle$  is the ground state for any value of  $\tilde{B}_2$ . From this, we obtain the expressions for the concurrence and singlet probability given in Eq. (7) of the main text.

Next, we derive general equations for the concurrence and singlet probability of a local probe coupled to a pseudospin in the critical regime of the  $B_c = 0$  transition. Equation (6) is a special case of this result.

The pseudospin effective Hamiltonian in this case is given by

$$\tilde{H}_{\text{cp}} = J_{12}\mathbf{S}_1 \cdot \mathbf{S}_2 + \tilde{J}_{2c}\mathbf{S}_2 \cdot \mathbf{S}_c - B_c S_{c,z}. \quad (27)$$

$S_{\text{tot},z} = S_{1,z} + S_{2,z} + S_{c,z}$  is again a good quantum number and we divide the full Hilbert space into subspaces with fixed  $S_{\text{tot},z}$  values. For  $S_{\text{tot},z} = \pm 3/2$ , there are two one-dimensional subspaces with eigenstates  $|S_{1,z}, S_{2,z}, S_{c,z}\rangle = |\uparrow\uparrow\uparrow\rangle$  and  $|\downarrow\downarrow\downarrow\rangle$ . The eigenenergies are  $E_{\pm 3/2} = (J_{12} + \tilde{J}_{2c})/4 \mp B_c/2$ , respectively. For  $S_{\text{tot},z} = 1/2$ , the subspace is three dimensional and the Hamiltonian matrix in the ordered basis  $\{|\uparrow\uparrow\downarrow\rangle, |\uparrow\downarrow\uparrow\rangle, |\downarrow\uparrow\uparrow\rangle\}$  is given by

$$H = \begin{pmatrix} \frac{J_{12} - \tilde{J}_{2c} + 2B_c}{4} & \frac{\tilde{J}_{2c}}{2} & 0 \\ \frac{\tilde{J}_{2c}}{2} & \frac{-J_{12} - \tilde{J}_{2c} - 2B_c}{4} & \frac{J_{12}}{2} \\ 0 & \frac{J_{12}}{2} & \frac{-J_{12} + \tilde{J}_{2c} - 2B_c}{4} \end{pmatrix}. \quad (28)$$

We can obtain the eigenvalues by solving the cubic function  $|H - \lambda I| = 0$ . The ground state energy in this subspace is

$$\lambda_1 = -\frac{1}{12} \left( J_{12} + \tilde{J}_{2c} + 2B_c + 2\sqrt{D_1} \cos \frac{\phi}{3} \right), \quad (29)$$

where  $\phi$  is defined in the range  $0 \leq \phi \leq \pi$  by

$$\cos \phi = \frac{D_2}{2D_1^{3/2}}, \quad (30)$$

$$\sin \phi = \frac{\sqrt{27\Delta}}{2D_1^{3/2}}, \quad (31)$$

and

$$D_1 = 4 \left( 4J_{12}^2 + 4\tilde{J}_{2c}^2 + 4B_c^2 - J_{12}\tilde{J}_{2c} + 4J_{12}B_c - 2\tilde{J}_{2c}B_c \right), \quad (32)$$

$$D_2 = 16 \left( 8J_{12}^3 + 8\tilde{J}_{2c}^3 - 8B_c^3 - 3J_{12}^2\tilde{J}_{2c} - 3J_{12}\tilde{J}_{2c}^2 + 6J_{12}\tilde{J}_{2c}B_c - 12J_{12}B_c^2 + 6\tilde{J}_{2c}B_c^2 + 12J_{12}^2B_c - 6\tilde{J}_{2c}^2B_c \right), \quad (33)$$

$$\Delta = \frac{1}{27} (4D_1^3 - D_2^2). \quad (34)$$

Without loss of generality, we will only consider  $B_c > 0$ . In this case  $B_c > 0$ , the ground state energy  $\lambda_1$  in the  $S_{\text{tot},z} = 1/2$  subspace is always lower than the ground state in the subspace with  $S_{\text{tot},z} = \pm 3/2$ . The corresponding eigenstate of the three-spin system is

$$|\Psi_{\text{GS}}\rangle = z_1 |\uparrow\uparrow\downarrow\rangle + z_2 |\uparrow\downarrow\uparrow\rangle + z_3 |\downarrow\uparrow\uparrow\rangle, \quad (35)$$

where

$$z_1 = -\frac{\tilde{J}_{2c}}{2\sqrt{Z}(F - \lambda_1)}, \quad (36)$$

$$z_2 = \frac{1}{\sqrt{Z}}, \quad (37)$$

$$z_3 = \frac{J_{12}}{2\sqrt{Z}(F + \lambda_1)}, \quad (38)$$

$$Z = \frac{\left(\frac{\tilde{J}_{2c}}{2}\right)^2 (\lambda_1 + F)^2 + \left(\frac{J_{12}}{2}\right)^2 (\lambda_1 - F)^2 + (\lambda_1^2 - F^2)^2}{(\lambda_1^2 - F^2)^2}, \quad (39)$$

$$F = \frac{J_{12} - \tilde{J}_{2c} + 2B_c}{4}. \quad (40)$$

As before, we construct the eight-dimensional density matrix for the ground state and trace out the pseudospin degree of freedom. The resulting reduced density matrix for the probe double dot is then given by

$$\rho = z_1^2 |\uparrow\uparrow\rangle\langle\uparrow\uparrow| + z_2^2 |\uparrow\downarrow\rangle\langle\uparrow\downarrow| + z_3^2 |\downarrow\uparrow\rangle\langle\downarrow\uparrow| + z_2 z_3 (|\uparrow\downarrow\rangle\langle\downarrow\uparrow| + |\downarrow\uparrow\rangle\langle\uparrow\downarrow|) \quad (41)$$

$$= \begin{pmatrix} z_1^2 & 0 & 0 & 0 \\ 0 & z_2^2 & z_2 z_3 & 0 \\ 0 & z_2 z_3 & z_3^2 & 0 \\ 0 & 0 & 0 & 0 \end{pmatrix}. \quad (42)$$

We can then compute the concurrence, which is given by

$$C = 2|z_2 z_3| = \frac{J_{12}}{Z|F + \lambda_1|}. \quad (43)$$

The singlet probability  $P_S$  is given by

$$P_S = \langle S | \rho | S \rangle = \frac{1}{2} (z_2 - z_3)^2 = \frac{1}{2Z} \left( 1 - \frac{J_{12}}{2(F + \lambda_1)} \right)^2. \quad (44)$$

We could obtain Eq. (6) of the main text by plugging  $B_c = 0$  into these expressions. However, the algebra is rather complicated. Here, we solve the effective Hamiltonian specifically for the case  $B_c = 0$ :

$$H = J_{12} \mathbf{S}_1 \cdot \mathbf{S}_2 + \tilde{J}_{2c} \mathbf{S}_2 \cdot \mathbf{S}_c. \quad (45)$$

Similar to the nonlocal probe case, we obtain the ground state

$$|\Psi_{GS}\rangle = \left( \frac{1}{\sqrt{2}} \cos \frac{\theta}{2} + \frac{1}{\sqrt{6}} \sin \frac{\theta}{2} \right) [|\uparrow\downarrow\uparrow\rangle - |\downarrow\uparrow\uparrow\rangle] - \sqrt{\frac{2}{3}} \sin \frac{\theta}{2} |\uparrow\uparrow\downarrow\rangle, \quad (46)$$

where  $\theta$  is defined in the range  $0 \leq \theta \leq \pi$  by

$$\cos \theta = \frac{J_{12} - \frac{\tilde{J}_{2c}}{2}}{\sqrt{J_{12}^2 - J_{12}\tilde{J}_{2c} + \tilde{J}_{2c}^2}}, \quad (47)$$

$$\sin \theta = \frac{\frac{\sqrt{3}}{2}\tilde{J}_{2c}}{\sqrt{J_{12}^2 - J_{12}\tilde{J}_{2c} + \tilde{J}_{2c}^2}}. \quad (48)$$

Calculating the reduced density matrix after tracing out the pseudospin degree of freedom, we obtain Eq. (6) of the main text.

---